

NEW GENERATION OF HIGH RESOLUTION ACOUSTIC IMAGING TECHNIQUE FOR MATERIAL CHARACTERIZATION AND NDT

R. Gr. Maev

DaimlerChrysler/NSERC Industrial Research Chair in Applied Solid State Physics and Material Characterization, University of Windsor, Windsor, Ontario, Canada

Abstract: This paper deals with the analysis of the novel high-resolution acoustic imaging NDE methods and technique for inspection the internal structure of the various materials and products, including different metals, alloys, composites, ceramics, multilayer structured materials, polymer blends, various joints, etc. The theoretical bases, as well as experimental fundamentals for quantitative characterization of the contrast response in the acoustic imaging are described together with overview of the recent results of the technical development in this field realized by different research groups. Together with mention in passing the well known methods, new techniques for the measurement of acoustical parameters will be discussed. This will include the $V(x, t)$ method, ultrasonic micro-spectrometry, air-coupling pair measurement technique for the reflection mode, as well as the $A(z)$ method for the transmission mode. Improvement of imaging resolution using higher harmonics is also one of the priorities to be addressed, including new opportunities for non-linear material characterization using parametric acoustic imaging. The last part of review is related to recent developments of high-resolution imaging techniques for practical uses for various industrial applications. New principles for rapid 2D and 3D image quantitative evaluation of bulk and sub-surface acoustical properties and microstructure based on a new concept of portable electronic system, together with matrix and phase array technique, will be reviewed. Based on the most successful experimental results, examples of different applications will be provided including evaluation of advanced material structure, quality control of joints, adhesive bonding, and layer structures, etc.

Introduction: The role of nondestructive materials characterization and evaluation (NDE) is changing and will continue to change dramatically. It has become increasingly evident that it is both practical and cost effective to expand the role of NDE and quality control to include all aspects of production and to introduce it as much as earlier in the manufacturing cycle. Today, and even increasingly in the future, using advanced optical, thermal, ultrasonic, laser-ultrasound, acoustic emission sensors, vibration, electro-magnetic, X-ray technique, etc., as well as modern measurement technique, along with signal/data processing, on-line information on the processing conditions can be continuously generated. Real-time process monitoring for more effective and efficient real-time control of various processes and as a result improved manufacturing quality control inspection and reliability will now become a practical reality. The new materials structures, joints, parts, components made from various materials demand the innovative applications of modern NDE techniques to monitor and control as many stages of the production process as possible. Simply put, intelligent advance manufacturing is impossible without integrating modern nondestructive evaluation into the production system.

Background: Acoustical imaging is well-known as a basic powerful research tool for studying the microstructure and properties of materials, and it has attracted the efforts of various research groups in different countries. Actually, high-resolution acoustic imaging, or acoustic microscopy is a relatively new technique for studying the microstructure of condense matters of a range of nature. The idea of a microscope using sound rather than light was first put forward by a Russian scientist (Sokolov, 1934). However, due to the limitations of existing technology, it was many years before high-resolution acoustic imaging was actually realized. The first prototype acoustic microscope was built forty years later in the USA, (C. Quate, Stanford University) in 1974. The advanced basic physical acoustics methods as well as various industrial applications of acoustic microscopy are still a developing field of study.

Quantitative Methods: The most popular quantitative technique in acoustic microscopy is the $V(z)$ -method [1, 2], in which the acoustic velocity and attenuation of leaky surface acoustic waves, as well as a reflectance function, can be determined from output signal V of the transducer, acquired as a function of the specimen displacement z . Together with the well known $V(z)$ method, we will introduce other techniques for the measurement of acoustical parameters. For quantitative materials characterization, acoustic methods employing separated transmitting and receiving transducers were developed, such as an ultrasonic micro-spectrometer with spherical-planar-pair lenses for the measurement of the reflection coefficient [3, 4]. The angular spectrum of the reflected wave in such system is determined by the rotation of the lens system as a whole, relative to the specimen surface. The ultrasonic system

with two transducers was also used for a measurement of the resonant transmission coefficient, [5] and for the determination of Lamb dispersion curves [6]. Obtaining the required data for the reconstruction algorithms occurred in two ways: one, the voltage of the output transducer was measured as a function of the lateral displacement of the transducer on the specimen's surface; or two, as a function of the frequency of the probing electrical tone burst pulse. A two-dimensional recording of the wave, scattered by the specimen, was proposed [7] for measuring elastic constants. The focus of the transmitting transducer in this method is placed on the specimen surface, but the scan plane of the receiver is located far from the focus. Thus, the recorded spatial distribution represents the angular spectrum of the reflected or transmitted wave. The angular resolution of the methods is determined by the spatial resolution of the receiver and the distance between the scan plane and focus. In previous articles [8, 9] we developed a new technique for measuring acoustical parameters called the A(z) method for the transmission mode. A new V(x) method was introduced later for the reflection mode [10, 11]. Both the A(z) and V(x) methods may include additional options, based on the air-coupling pair measurement technique for both the reflection mode, and for the transmission mode.

The V(Z) Method: The most popular quantitative technique in acoustic microscopy is the V(z) method, in which the acoustic velocity and attenuation of leaky surface acoustic waves, as well as a reflectance function, can be determined from the output signal V of the transducer acquired as a function of specimen displacement z. In most of these systems, the output voltage V(z) of the focused transducer is recorded as a function of the distance between the focus and the surface of the specimen [1, 2] and [12–15]. The phase velocity and propagation attenuation of leaky surface acoustic waves (LSAW), as well as a reflectance function for the specimen-liquid coupling interface, can be obtained from the recorded amplitude data. In the V(z) system (Fig. 1a), the LSAW is generated by a ray incident on the liquid-solid interface at the critical angle θ_R . The surface wave propagates along the interface reradiating (“leaking”) back to the liquid at the same angle θ_R . If the transducer is moved toward the specimen, one of the reradiated rays (ray R) is effectively received by the transducer. Only a leaky wave whose critical angle is less than the half-aperture angle of the transducer $\theta_R < \theta_m$ can be excited and detected in this scheme.

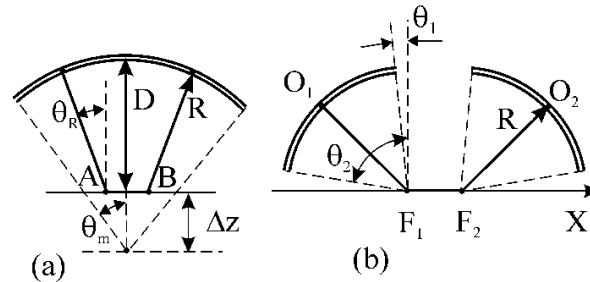


Figure 1. Ray models of the (a) V(z) and (b) V(x) material characterization systems

The time delay Δt between the responses to the ray R and the directly reflected ray D is related to the velocity of the LSAW, C_R [16, 17]:

$$C_R = \left[\frac{\Delta t}{C \cdot \Delta z} - \frac{1}{4} \cdot \left(\frac{\Delta t}{\Delta z} \right)^2 \right]^{-1/2}$$

where C is the sound velocity in the liquid and Δz is the defocusing distance. Obviously, the accuracy of the LSAW measurement increases with increasing Δz . The maximum value of Δz is limited by the focal distance F of the lens and the half-aperture angle θ_m : $\Delta z < F \cdot \cos(\theta_m)$. Usually, the maximum value of F is limited by the sound attenuation in the liquid. On the other hand, it is possible to obtain better accuracy by decreasing θ_m , but this is not desirable because of the reduction in the critical angle range.

A point-focus-beam acoustic lens was used in the first implementation of the V(z) technique for an isotropic specimen study [2]. For the characterization of anisotropic materials, a line-focus-beam acoustic lens was proposed [12]. A Lamb wave lens and directional lenses with noncircular shaped transducers [13] were developed to obtain enhanced sensitivity for particular ranges of incident or orientation angles. As well, various electrical exciting

waveforms and processing electronics were employed for $V(z)$ data acquisition. The conventional UMC system works in a tone burst mode and the amplitude of $V(z)$ is only used for analysis. The amplitude and the phase of the output voltage were recorded to reconstruct the reflectance function by the Fourier transform of the complex $V(z)$ [14]. A continuous wave Doppler system produces a complex $V(z)$ for a single, particular frequency [10, 18]. Conversely, the $V(z, t)$ waveform acquired in the pulse mode represents the properties of the specimen over a wide frequency band [19, 20]. With all of these techniques, the accuracy of the measured LSAW parameters and the incident angle resolution increases with the growing amount of $V(z)$ data [14]. However, the maximal defocusing distance is limited in the $V(z)$ configuration by the geometry of the acoustic lens. Furthermore, the wave velocity in water is used as reference in the $V(z)$ schemes. Due to the temperature dependence of the wave velocity in water, the error in the temperature measurement significantly affects the accuracy of the measured velocity and attenuation of LSAW [1, 15, and 28].

Micro-Spectrometry: Several ultrasonic systems employing two transducers have also been developed for quantitative material characterization. In an ultrasonic micro-spectrometer, spherical-planar-pair lenses were used for the measurement of the reflection coefficient over a wide frequency range [3], [4]. An angular spectrum of the reflected wave is detected in this system by tilting the spherical-planar-pair lenses as a unit. The size of the planar transducer is large enough to provide sufficient angular selectivity and, because of geometrical restrictions, the measurements can not be carried out at small and large angles of incidence (see Figure 2).

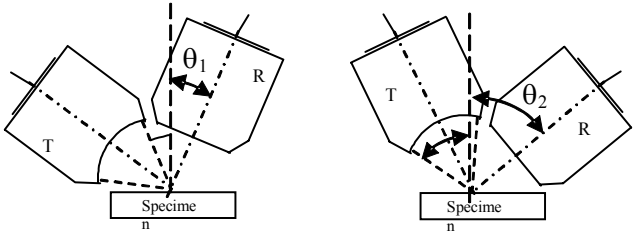


Figure 2. Experimental setup for ultrasonic angular micro-spectrometer with Spherical-Planar Pair lenses. Incident angle $\theta_1 < \theta < \theta_2$.

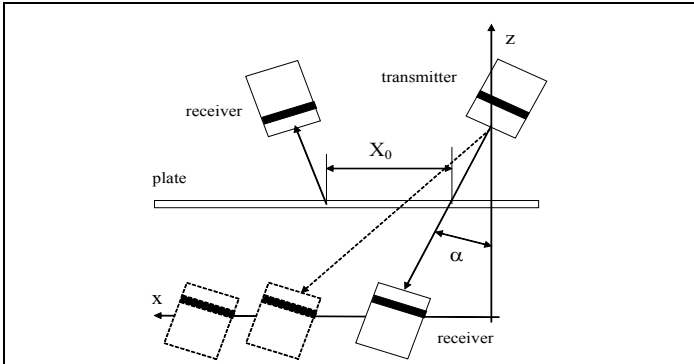


Figure 3. Experimental setup for air coupling pair system. Due to the narrow directivity of the transducers, additional monitoring of angle α is used

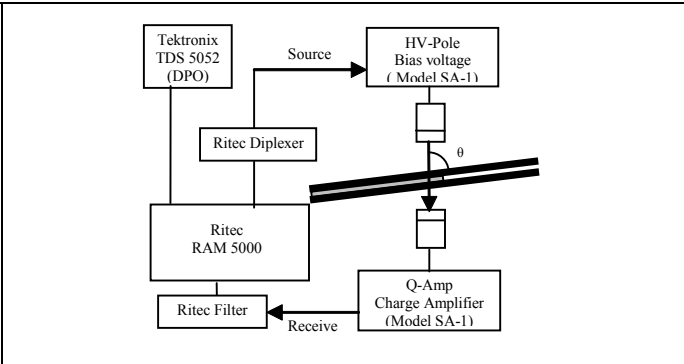


Figure 4. Air-Coupling pair measurements. The lap joints are placed in between the transducers with angle $\theta = 8^\circ - 12^\circ$. Frequency of burst is equal 500 kHz

An ultrasonic system employing separated transmitting and receiving point-focus transducers has been developed to study the anisotropic propagation of LSAW. During the experiments [21, 22], the foci were located on the surface of the specimen at a fixed distance, and the specimen was rotated to obtain the group velocity of surface waves as a function of the propagation angle. In systems [23–25], the focus of the transmitter was located on the liquid–solid interface, but the recording of the scattered acoustic field was carried out by two-dimensional scanning of the receiving transducer. The recorded spatial distribution represented the angular spectrum of the scattered wave associated with the reflectance or transmission coefficients. Thus, using this technique, the angular resolution

was restricted by the spatial resolution of the receiver and the distance from the point source to the plane of the data acquisition [26]-[27].

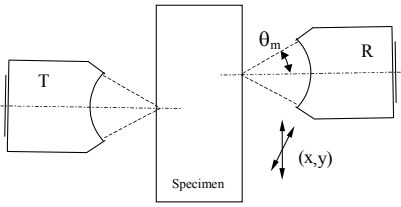


Figure 5. Through transmission mode. The angular resolution in this method is determined by the spatial resolution of the receiver and the distance between scan plane and focus. The incident angle is $\theta < \theta_m$

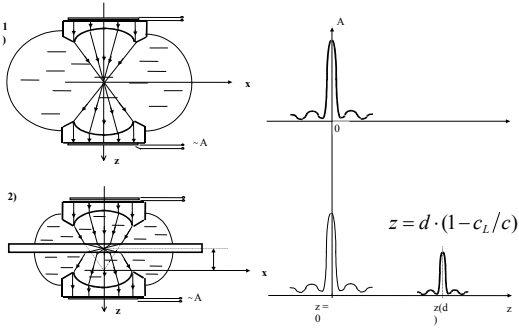


Figure 6. $A(z)$ method for quantitative measurements in through transmission

The ultrasonic system with two transducers was also used for a resonant transmission coefficient measurement and for the determination of Lamb dispersion curves [6]. Lateral scanning of the receiving air coupling transducers along with surface of the specimen was used to acquire Lamb wave measurements and to study the properties of the materials in plate form.[5, 25] (see Figures 3 and 4). Obtaining the required data for the reconstruction algorithms occurred in two ways, one—the voltage of the output transducer was measured as a function of the lateral displacement of the transducer on the specimen’s surface, or two—as a function of the frequency of the probing electrical tone burst pulse. However, the transducers had narrow directivity functions and monitoring of the transducer angles was employed to acquire a complete data set. A two-dimensional recording of the wave, scattered by the specimen, was proposed for measuring elastic constants in papers [7]. A two-dimensional Fourier transformation of the acquired time-spatial data represented the wave number dispersion curves. Due to the high directivity of the transducers employed in the experiments, the single scan data corresponds to a narrow range of the angles of incidence [25]. To obtain dispersion curves for the entire angular range, the data acquisition and processing should be repeated many times at different angular orientations of the transducers (Figure 5). Another system with highly focused probes has been developed for rapid dispersion curve mapping [23] [24], because of the large angular aperture of the transducers, only a single scan is necessary to acquire the complete data set.

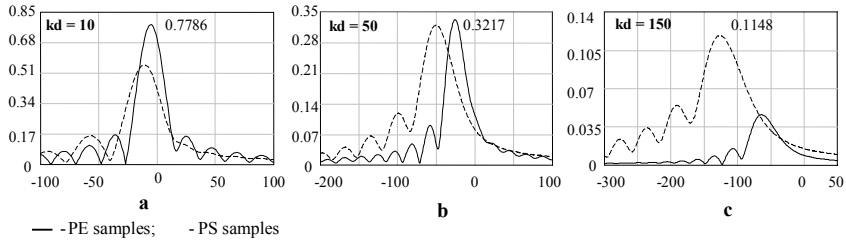


Figure 7. Application of $A(z)$ method for polymer study: $A(kz)$ curves for polyethylene and polystyrene samples with thickness $kd = 10$ (a), $kd = 50$ (b) and $kd = 150$ (c). The peak shift from the point of $z = 0$ is proportional to the specimen thickness d and depends on the sound velocity ratio – the larger the shift, the bigger the ratio.

The $A(z)$ Method: The $A(z)$ method relies on the dependence of the output signal $A(z)$ on the distance z between the receiving and radiating lenses in the two-lens focusing system of the transmission acoustic microscope [8, 9]. Without an object the output signal is at its maximum when the focuses of both lenses coincide (confocal position). Displacing one of the lenses causes signal decay and oscillations due to the interference of the signals produced by different parts of the beam in the receiving transducer (Figure 6). When an object such as a plate with thickness d , is placed in the path of the focused beam, its focus is shifted due to the refraction of a convergent beam in the plate.

To reach the maximum of the signal, it is necessary to change the distance between the lenses. A maximum arises with a new confocal position (Figure 6). Applying a well-known formula of the ray optics the lens shift z can be expressed as: $z = d(1 - C_L/C)$, where C_L and C are ultrasound velocities in an object and in a coupling liquid, respectively. Measuring the specimen thickness d and the shift z of the receiving lens, we can determine the ratio C_L/C and, finally, a value of C_L . Measuring the ratio of maximums on both of the $A(z)$ plots, before placing an object and after it, makes it possible to find a value of the transmission coefficient and then to estimate the attenuation in a specimen. An earlier theoretical model for the $A(z)$ method was developed in [9] and experimentally this method has been applied to measuring acoustic parameters of some polymer, polymer blends (see Figure 7) and biological samples [8].

The $V(x, t)$ Method: $V(x, t)$ is a newly developed time-resolved, pair lenses, line-focused method based on the lateral scanning of the receiving transducer. It was shown theoretically [10, 11] that the output voltage $V(x, t)$ of the system is related by the Fourier transform to the product of the reflectance coefficient and the transfer function. In the $V(x)$ scheme, the tilted transmitting and receiving transducers are used in a pitch-catch arrangement, and the receiver is translated along the interface in the x direction (Figure 1, (b)). The velocity of the non dispersive LSAW is simply the ratio of the travel distance Δx and the relative time delay Δt of the leaky wave R : $C_R = \Delta x / \Delta t$. Due to the geometry of the $V(x)$ system, the range of angles of incidence (θ_1, θ_2) can be made close to the values $(0, \pi/2)$, and there is no restriction on the maximum scanning distance Δx in the direction of the LSAW propagation. For an ideal uniform temperature distribution in the immersion liquid (see Figure 8), the time of flight in the liquid $\Delta t^* = (O_1F_1 + F_2O_2) / C$ is constant during data acquisition. Also, Δt^* remains constant if the temperature distribution along the rays O_1F_1 and F_2O_2 does not change during the scan of the receiving transducer. Under this sufficient condition, the relative time delay Δt is only associated with the LSAW velocity, and the temperature coefficient η_x of the CR measurement error is negligible. It is difficult to estimate theoretically the value of η_x , but below we have presented the results of the experimental study of the temperature stability of the $V(x)$ scheme

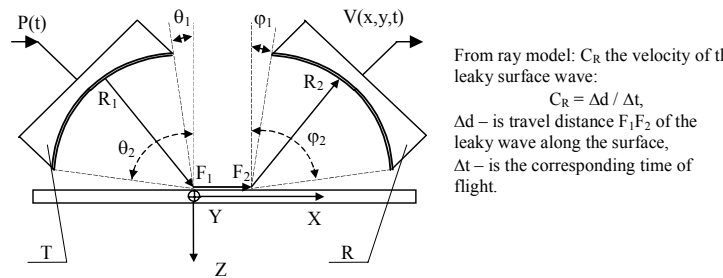


Figure 8. Physical principles of $V(x, t)$ method

The proposed method was illustrated experimentally by measurements of the velocities of leaky Rayleigh, Lamb, and longitudinal skimming waves [28]. Some results for the materials with known properties were tested using the experimental setup described in Figure 8. The complex reflectance function for the water-lead interface is similar for all angles of incidence because of the high density and low elasticity of lead. In previous work, [11, 28] a new time-resolved, line-focused UMC system was developed based on lateral scanning of the receiving transducer; it was shown theoretically that the output voltage $V(x, t)$ of the system is related by the Fourier transform to the product of the reflectance coefficient and the transfer function. In comparison with the $V(z)$ system, the geometry of the $V(x)$ scheme does not restrict the scanning distance and the aperture angle. The measurements of the LSAW velocity carried out using fused quartz over a wide temperature range show good temperature stability of the measurements employing the $V(x)$ technique. The angular resolution of the $V(x, t)$ system was analyzed using the ray model and wave theory. In comparison with the $V(z)$ system, the geometry of the $V(x)$ scheme does not restrict the scanning distance and the aperture angle. The proposed method was illustrated experimentally by measurements of the velocities of leaky Rayleigh, Lamb, and longitudinal skimming waves. The experimental results obtained for the metal, crystal, ceramic, and polymer specimens are in good agreement with published data. The measurements of the LSAW velocity carried out using fused quartz over a wide temperature range show good temperature stability of the measurements employing the $V(x)$ technique.

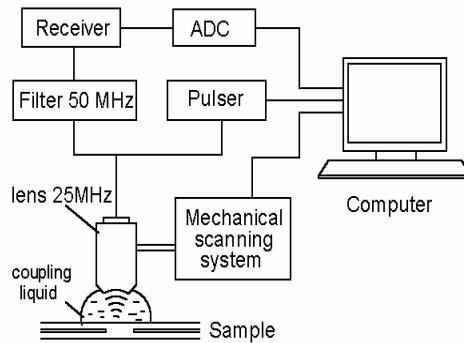


Figure 9. Schematic diagram of the scanning acoustical microscope as used for second harmonic imaging

Second harmonic mode of the acoustical microscope: The signal of the second harmonic, generated by nonlinear reflection, in most cases is 30–50 dB weaker than the signal of fundamental frequency, requiring careful selection of the experimental parameters. A single, short sound pulse is usually used in the acoustical microscope to maximize the spatial resolution. The wide-band spectrum of such a pulse contains strong components at double frequency. As well, the bulk nonlinearity of all the acoustical components of the microscope and object, especially of the coupling liquid, produce uninteresting second harmonic waves, which accompany the waves of the fundamental frequency. These waves will therefore contribute to the image at second harmonic, identical information to that already found in the linear picture [19]. In [20] this idea was experimentally demonstrated for the resolution of weak-reflecting inclusions, using a scanning microscope with a 25 MHz acoustical focusing lens. A selective filter-amplifier with a basic frequency of 50 MHz and a bandwidth 4 MHz was included into the receiving branch (see. Figure 9).

The sound wave was excited by applying to the lens transducer a single pulse with amplitude of 120 V and duration of 16 nS. Without taking any specific action to enhance the second harmonic, its level in the received signal lies at approximately 25 dB (measured during reflection from the surface of a steel plate in beam focus). By decreasing the receiver bandwidth, the tone burst of the second harmonic has a significantly longer duration compared to that without frequency selection. This leads to the deterioration of the spatial resolution in depth up to 0.5–0.7 mm.

The C-scan image is generated by mechanical raster scanning of an area up to 40×40 mm along the surface with steps of 0.05–0.01 mm. Figure 10 presents the scans of such a specimen: two galvanized steel sheets with thickness 2 mm, joined by a resistance spot weld. To exclude any aberration due to non-planar surface conditions, the indentation from the weld electrode was removed by milling. The dark spot in the center of the pictures is the weld nugget. The sound can freely pass through it and only some reflecting inhomogeneities are visible as light points.

The bright area outside the weld corresponds to the free internal surface of the upper sheet with practically 100% sound reflection. Between these regions lies a grey ring, corresponding to a zone with poor acoustical contact. It is known that in this zone melted zinc accumulates during the welding process, and creates a lot of connecting stalactite-stalagmite type structures. Such a micro rough connective layer should be a very good source of contact acoustical nonlinearity. Since the thickness of this layer and the size of these microstructures are much less than a wavelength, they will contribute in an integral way. Indeed, the second harmonic picture shows this region as a bright white ring. The amplitude of the second harmonic in this region is at least ten times bigger than that of the other regions.

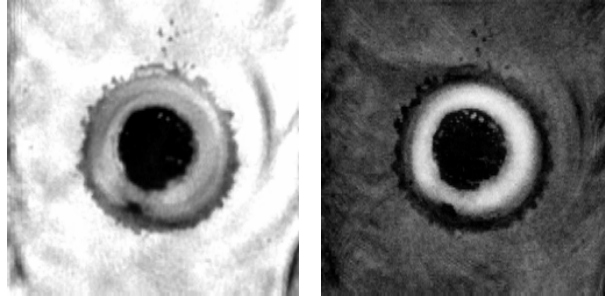


Figure 10. C-scans of spot weld, obtained on fundamental frequency (left) and on second harmonic (right). Size of scanned region is 12×12 mm.

2D Matrix Transducer: Matrix and array transducers offer several enhanced capabilities in imaging and beam forming compared to a single transducer scanning system. The matrix transducer technology makes fast data acquisition and imaging possible, while using motionless transducers. Advanced technologies such as micro-machining and IC manufacturing can produce matrices of thousand elements of less than 0.1 mm in size, creating an acoustic analog of CCD camera [29, 31]. This size is essential for phased arrays; given the element size must be around half a wavelength for efficient beam-forming [30]. However, for matrices not using phased principles to build the acoustic beam, such small elements represent a disadvantage. Matrix transducers having such a high density can only operate in the pick-up mode due to power dissipation restrictions. Moreover, acoustic wavelengths at megahertz frequencies are at least 100 times larger than the light wavelengths, thus, there seems to be no reason to go down to the micron range resolution [32]. One of the array transducers used in one of our device has the diameter of 10.0 mm and contained 52 emitting-receiving broadband elements with the central frequency around 20 MHz. Experimental data have been acquired with a miniaturized original ultrasonic pulser-generator PC board and, digital data are transferred to the portable PC. All analog settings are maintained constant through the experimental procedure. The sampling rate used in the experiments was 500 MSamples/s. For image smoothing and quality enhancing various 2D interpolation algorithms are used. The imaging capability of the system generally depends on the penetration depth of the transducer. The penetration depth drops with the decreasing size of the element due to the beam divergence and the increasing electrical mismatch with 50 Ohms transmitters and receivers. In general the image quality gets worse for smaller and deeper reflectors.

High-Resolution Ultrasonic Inspection Methods for Joint Inspection: The traditional methods of any joints monitoring are combinations of visual inspection, pry testing and destructive tests, like in the resistance spot welds, with hammer and chisel. The only effective non-destructive method has been the ultrasonic pulsed echo technique based on an evaluation of ultrasonic echo patterns in a specimen. The current ultrasound technique is capable of determining the approximate parameters of the joint. Disadvantages of that technique and method are evident: a wide range of ambiguity in treating echograms; a high sensitivity of the result to the alignment of the transducer perpendicular to the surface; the dependence of the results on operator experience and skill; the impossibility of building the method into an on-line process; etc.

Because of that, the hottest NDE problem today is development of new high-resolution inspection systems of various advanced materials and joints, like rivets, different kind of welding, such as laser, MIG and ARC-welds, resistant spot welds, with the goal to implement this new coming generation of industrial prototype of automated acoustic, miniaturized, hand-held inspection device on the industrial shop floor and to be able to perform the desired non-destructive inspection functions during manufacturing process as well as maintenance services.

Using acoustic imaging systems with short probe pulses provides a way to visualize small-scale failures of contact and other defects at different depths. For spot welding acoustic imaging systems makes it possible to inspect fine details of internal areas of joints in spite of the curved outer surfaces of welding spots.

To show the potential of high-resolution acoustic imaging technique we used a wide-field short-pulse acoustic microscope (see Fig. 9). The method was applied to evaluation of spot-welding joints of two steels sheets 1-2 mm thick of each. In spite of the fact that the top surface of specimen was distributed by welding, high quality acoustic images of the nugget zone were obtained. The C-scan and B-scan images contain well-shaped defects of joints and the confirm power of the method for NDE and QC of spot-welded joints (see Fig.10). The combination of the C-

scan and the B-scan images in one picture can give a real 3D image of the defect distribution inside the welding zone, which can be also very useful from a technological point of view.

The current results of this study show that high-resolution acoustic imaging technique can be successfully applied in spot welding as an effective inspection method to detect any kind of defects, and can be used for manufacturing welding quality control. Acoustic imaging methods based on acoustic visualization and characterization are extremely promising also for laser welds and rivet joints quality evaluation. This technique can provide total bulk reconstruction of the joint zone, including the topography of the top and bottom faces, the structure of the interface between the sheets, and any expulsions, voids, pores, cracks or other defects in the welding zone. The applications of new acoustic imaging portable technology, now in active development, have the potential to transform the whole NDE area by intrinsically changing smart NDE process.

Conclusions: During the last two decades, the high resolution acoustic imaging has become an effective instrument for the investigation of the internal structure of materials and for industrial non-destructive evaluation. At the same time, quantitative acoustic imaging research was mostly applied in high resolution acoustic microscopy in material sciences and also in biomedical imaging. Further improvement of the quantitative methods may be realized using other types of ultrasonic-media interactions and, accordingly, provide additional specific information about the object. The quantitative NDE acoustical imaging technique and methods would enhance its capability for the material characterization and imaging of cracked micro-inhomogeneities, crucial for the integrity of high-damage risk materials and products used in NDE aviation, automotive and nuclear power industries as well as microelectronics.

Acknowledgment: I acknowledge the National Science and Engineering Research Council of Canada (NSERC) and DaimlerChrysler Corporation for funding this work. I would also like to thank my colleagues from other research groups, whose results were included in this review paper (see references), in particular I would like to thank my research team for their help and significant contribution to this review paper, including my research associates Drs. S. Titov, F. Severin, E. Maeva, and my students and PDF.

References:

- [1] A. Briggs, Acoustic microscopy, Oxford, Clarendon Press, 105–152, 1992.
- [2] R. Weglein and R. Wilson, “Characteristic material signature by acoustic microscopy”, *Electron. Lett.*, 14, 352–354, 1978.
- [3] N. Nakaso, K. Ohira, M. Yanaka Y. Tsukahara, “Measurement of acoustic reflection coefficients by an ultrasonic microspectrumeter”, *IEEE Trans. Ultrason. Ferroelec. Freq. Contr.*, 41, 494–502, 1994.
- [4] N. Nakaso, Y. Tsukahara and N. Chubachi, “Evaluation of spatial resolution of spherical–planar–pair lenses for elasticity measurement with microscopic resolution”, *IEEE Trans. Ultrason. Ferroelec. Freq. Contr.*, 43, 422–427, 1996.
- [5] O. Lobkis, D. Chimenti, “Three–dimensional transducer voltage in anisotropic materials characterization”, *J. Acoust. Soc. Amer.*, 106, 36–45, 1999.
- [6] T. Kundu, A. Maji, T. Ghosh, and K. Maslov, “Detection of kissing bonds by Lamb waves”, *Ultrasonics*, 35, 573–580, 1998.
- [7] R. Smith, D. Sinclair and H. Wickramasinghe, “Acoustic microscopy of elastic constants” in *Proceeding Ultrasonic Symp.*, 677–682, 1988.
- [8] R. Gr. Maev, “Scanning acoustic microscopy of polymeric and biological substances”, *Tutorial Archives of Acoustics, Poland*, 13, N 1-2, 13–43, 1988.
- [9] R. Gr. Maev, V.M. Levin, “Principles of local sound velocity and attenuation measurements using transmission acoustic microscope”, *IEEE Trans. Ultrason. Ferroelec. Freq. Contr.*, 44, N6, 1224, 1997.
- [10] R. Gr. Maev, S.A. Titov, “Measurement method based on scanning Doppler continuous wave acoustic microscope”, *Topics on Nondestructive Evaluation Series*, 3, ASNT Publication, 343-350, 1998.
- [11] S. Titov and R. Maev, “V(X,T) acoustic microscopy method for leaky surface acoustic waves parameters measurements”, *Proc. IEEE Ultrason. Symp.*, 607–610, 2000.
- [12] J. Kushibiki and N. Chubachi, “Material characterization by line–focus–beam acoustic microscope”, *IEEE Trans. Sonics and Ultrasonics*, SU–32, 189–212, 1985.
- [13] A. Atalar, H. Koymen, A. Bozkurt and G. Yaralioglu, “Lens geometries for quantitative acoustic microscopy”, in book *Advances in acoustic Microscopy*, 1st, New York: Plenum Press, 117–151, 1995.

- [14] K. Liang, G. Kino and B. Khuri-Yakub, "Material characterization by the inversion of $V(z)$ ", IEEE Trans. Sonics and Ultrasonics, SU-32, 213–224, 1985.
- [15] K. Kushibiki, Y. Ono, Y. Ohashi and M. Arakawa, "Development of the line-focus-beam ultrasonic material characterization system", IEEE Trans. Ultrason. Ferroelec. Freq. Contr., 49, 99–113, 2002.
- [16] K. Yamanaka, "Surface acoustic waves measurements using an impulsive converging beam", J. Appl. Phys., 54, N 8, 4323–4329, 1983.
- [17] D. Xiang, N. Hsu and G. Blessing, "The design, construction and application of a large aperture lens-less line-focus PVDF transducer", Ultrasonics, 34, N 6, 641–647, 1996.
- [18] S. Titov and R. Maev, "Doppler continuous wave scanning acoustic microscope", Proc. of IEEE Ultrason. Symp., 713–718, 1997.
- [19] Y. Lee and S. Cheng, Measuring Lamb dispersion curves of a bi-layered plate and its application on material characterization of coating. IEEE Trans. Ultrason. Ferroelec. Freq. Contr., 48, 830–837, 2001.
- [20] Yongping Zheng, Roman Gr. Maev, Igor Yu. Solodov, "Nonlinear acoustic applications for material characterization: A review", Canadian Journal of Physics, Vol. 77, No 12, pp.927-968, 1999
- [21] R. Vines, S. Tamura and J. Wolfe, "Surface acoustic wave focusing and induced Rayleigh waves", Phys. Rev. Lett., 74, 2729–2732, 1995.
- [22] A. Every, A. Maznev and G. Briggs, "Surface response of a fluid loaded anisotropic solid to an impulsive point source: application to scanning acoustic microscopy", Phys. Rev. Lett., 79, N13, 2478–2481, 1997.
- [23] M. Hauser, R. Weaver and J. Wolfe, "Internal diffraction of ultrasound in crystals: phonon focusing at long wavelengths", Phys. Rev. Lett., 68, N 17, 2604–2607, 1992.
- [24] M. Pluta, M. Schubert, J. Jahny and W. Grill, "Angular spectrum approach for the computation of group and phase velocity surface of acoustic waves in anisotropic materials". Ultrasonics, 38, 232–236, 2000.
- [25] D. Alleyne and P. Cawley, "A two-dimensional Fourier transform method for the measurement of propagating multimode signals", J. Acoust. Soc Am., 89, 1159–1168, 1991.
- [26] D. Fei and D. Chimenti, "Rapid dispersion curve mapping and material property estimation in plates", Review of Progress in QNDE, 1368 – 1375, 2000.
- [27] D. Fei and D. Chimenti, "Complex transducer point model of focused-beam property estimation in plates", Review of Progress in QNDE, 1377 – 1384, 2001.
- [28] Titov S.A., Maev R.G. and Bogachenkov A.N. (2003) "Wide-aperture, line-focused ultrasonic material characterization system based on lateral scanning", IEEE Trans. Ultrason. Ferroelec. Freq. Contr., 50, N8, pp.1046-1056, 2003.
- [29] K. Erikson, A. Hairston, A. Nicoli, J. Stockwell, and T. White, "A 128×128 ultrasonic transducer array", in: Proc. IEEE Ultrasonics Symp., Vol. 2, eds. S.C. Schneider and B.R. McAvoy, IEEE, NY, 1625-1631, 1997.
- [30] D.H. Turnbull, "Two-Dimensional Transducer Arrays for Medical Ultrasonic Imaging", Ph.D. Thesis, University of Toronto, 1992.
- [31] W.R. Davis, B. Lasser, "Real-time Ultrasonic Imaging Using CCD Camera Techniques", in Proc.11 Intern. Symp. For Nondestructive Characterization of Materials, Springer, Berlin, pp.135-141, 2002
- [32] R. Gr. Maev, A. Ptchelintsev and A. Denisov, "Acoustical imaging using matrix of piezoelectric transducers for nondestructive evaluation of plastic composites", in: Proc. ICCE, p. 665, ICCE, Orlando, 1999.